Tuning bio-aerogel properties for controlling theophylline delivery. Part 1: Pectin aerogels

Sophie Groult, Sytze Buwalda, Tatiana Budtova

Submitted 1 February 2021 Materials Science and Engineering C

Revised 3 April 2021

Tuning bio-aerogel properties for controlling theophylline delivery.

Part 1: Pectin aerogels

Sophie Groult, Sytze Buwalda, Tatiana Budtova*

MINES ParisTech, PSL Research University, Center for Materials Forming (CEMEF), UMR CNRS 7635, CS 10207, 06904 Sophia Antipolis, France

*Corresponding author: Tatiana Budtova

Tatiana.budtova@mines-paristech.fr

Abstract

A comprehensive study of release kinetics of a hydrophilic drug from bio-aerogels based on pectin was performed. Pectin aerogels were made by polymer dissolution, gelation (in some cases this step was omitted), solvent exchange and drying with supercritical CO_2. Theophylline was loaded and its release was studied in the simulated gastric fluid during one hour followed by the release in the simulated intestinal fluid. Pectin concentration, initial solution pH and concentration of calcium were varied to tune the properties of aerogel. The kinetics of theophylline release was monitored and correlated with aerogel density, specific surface area, and aerogel swelling and erosion. Various kinetic models were tested to identify the main physical mechanisms governing the release.

Keywords: pectin; aerogel; drug release; theophylline, kinetics; specific surface area

1. Introduction

Bio-aerogels are dry, highly porous and ultra-light polysaccharide materials with a very high internal pores' surface area (several hundreds of m^2/g) [1-4]. Most of them, except aerogels based on nanocellulose, are prepared via polymer dissolution, gelation or direct non-solvent induced phase separation and drying with supercritical (sc) CO_2 [1, 3, 5]. The latter allows avoiding pore collapse, which may occur during drying at ambient pressure, and keeping the morphology of the dry material similar to that of the gel. Because of their unique properties, bio-aerogels are attractive materials for numerous applications such as thermal and acoustic insulation, catalyst support, fuel cells, capacitors, absorption and adsorption, and food packaging [1, 4-6]. Recently, bio-aerogels have also emerged as controlled drug delivery systems [7-10], which aim at the localized and sustained release of therapeutic agents, decrease the number of drug administrations and protect the drug from (enzymatic) degradation. By tuning and controlling synthesis conditions, bio-aerogels potentially allow for high drug loadings [11]. In addition, bio-aerogels may increase the bioavailability of low solubility drugs, improve drug stability and allow for a precise control over the release kinetics. Furthermore, aerogels hold promise for wound dressing applications [12].

Among the various polysaccharides, pectin, a polyelectrolyte found abundantly in the cell walls of plants and in fruits, is particularly interesting for biomedical applications such as drug delivery because of its biodegradability, biocompatibility, bioactivity as well as its gelling and stabilizing abilities [13]. Pectin is composed of a linear chain of galacturonic acid units, branched with ramnosyl units and neutral sugars. The galacturonic acid units can be methyl esterified, defining a degree of esterification (DE). The gelation of pectin solutions depends on various parameters, including pectin concentration, temperature, pH and concentration of metal ions. Below the pKa of pectin (3.0-3.5) [14], and depending on the polymer concentration, physical gelation may occur at room temperature due to hydrogen bonds between hydroxyl and protonated carboxyl groups as

well as hydrophobic interactions between methyl ester groups [15, 16]. Above the pKa, the addition of divalent cations, such as calcium ions, may lead to the gelation of pectin solutions due to the formation of intermolecular junction zones via ionic bonds following the 'egg-box' model [17]. In this case, the deprotonated acid moieties of galacturonic acid units interact with divalent cations and create strong intermolecular ionic bridges. Pectin is gastro-resistant, which facilitates the potential use of pectin aerogels in oral drug delivery applications. In addition, the preparation conditions of pectin solutions and gels can be varied widely, which allows for a broad range of aerogel morphologies and properties.

A limited number of publications report on pectin aerogels for drug delivery purposes. Pectin aerogel beads of millimeter size for the release of antibiotic and anti-inflammatory drugs were made via a prilling technique [18] and via dropping a pectin solution into a metal ion salt solution [19]. Also, sub-millimeter sized pectin [20] and pectin-alginate hybrid [21] aerogel microspheres for the release of the anti-inflammatory drug ketoprofen were prepared via an emulsion-gelation technique. Horvat et al. prepared pectin-xanthan hybrid aerogel coatings for the release of the non-steroidal anti-inflammatory drugs diclofenac sodium and indomethacin [22]. Tkalec et al. [23] and Horvat et al. [24] investigated pectin aerogel monoliths for the release of the poorly water-soluble drug nifedipine. Pantic et al. [25] prepared pectin monoliths for the release of the multifunctional compound curcumin, which is used as food additive, in cosmetics and as potential drug. Veronovski et al. reported on the release of the hydrophilic model drugs theophylline and nicotinic acid from apple and citrus pectin aerogel monoliths and multi-layer aerogel beads that were crosslinked with Ca^{2+} ions [26]. The more sustained release from citrus pectin aerogels compared to apple pectin aerogels was ascribed to the lower DE in citrus pectin, resulting in longer degradation times and reduced release rates.

Despite the information available in the existing reports on pectin aerogel drug carriers, as described above, an in-depth understanding correlating release kinetics and aerogel properties is still missing. For example, it was shown that pH of pectin starting solution and the concentration of calcium ions strongly affect aerogel density and specific surface area [27]. However, it is unclear whether these properties of the starting solution influence drug release kinetics and how. Also, a correlation between pectin aerogel properties, swelling and dissolution in simulated gastric and intestinal fluid and release properties should be established. Furthermore, a model should be selected that can be used to describe release kinetics. Addressing these issues is a prerequisite for tuning aerogel properties towards desired drug release applications.

The goal of this work is to study the release of a model hydrophilic drug, theophylline, from different pectin aerogel matrices in order to establish structure-properties correlations which can explain drug release mechanisms. For this purpose, structural and physico-chemical properties of the pectin aerogel carrier were systematically varied by adjusting the preparation conditions and gelation mechanisms (pectin concentration, calcium concentration, pH of pectin solution). Aerogel swelling, erosion and drug release profiles from different matrices were characterized and correlated. Kinetics models were used to identify the main physical mechanisms governing the release. The results obtained in this model study will be further used in the upcoming publications on the release properties of pectin-organic (cellulose) and pectin-inorganic (silica) aerogels.

2. Experimental section

2.1 Materials

Citrus pectin with a degree of esterification of 35% (as specified by the provider) and molecular weight 1.15 10^5 g/mol (as determined in ref [28]) was kindly donated by Cargill. Calcium chloride ($CaCl_2$) was from Acros Organics. Ethanol, potassium dihydrogen phosphate (KH_2PO_4), potassium

hydroxide (KOH), sodium hydroxide (NaOH) and hydrochloric acid (HCl, 32%) were from Fisher Scientific. Theophylline (purity > 99%) was from Acros. All products were used as received. Simulated gastric fluid without enzymes (SGF) was prepared from HCl solution (0.1 N, pH 1.0) and simulated intestinal fluid without enzymes (SIF) (pH 6.8) was made using NaOH at 11 mM (0.65 g/L) and KH_2PO_4 at 50 mM (6.8 g/L). Water was distillated.

2.2 Methods

2.2.1 Preparation of theophylline-loaded pectin aerogels

Pectin aerogels were prepared as described previously [27] via dissolution – gelation (in some cases gelation did not occur) – solvent exchange – drying with sc CO_2 (Figure 1). Pectin solutions were made by dissolution of pectin powder in distilled water at 65 °C under stirring at 400 rpm. Concentrations are given in weight percent (wt %). After complete dissolution, solution pH was adjusted by adding a small quantity of HCl or KOH. Pectin solutions were then poured into molds of 27.5 mm in diameter. In certain cases, $CaCl_2$ was added under stirring. The molar ratio R of Ca^{2+} ions to pectin carboxyl groups was calculated as follows:

$$R = \frac{[Ca^{2+}]}{[COO^-]} \quad (1)$$

Pectin solutions were let at rest for 48 h at room temperature. Depending on the conditions (concentration, pH, presence of $CaCl_2$) solutions were gelling or not as determined via the vial tilting test (solution flowing or not).

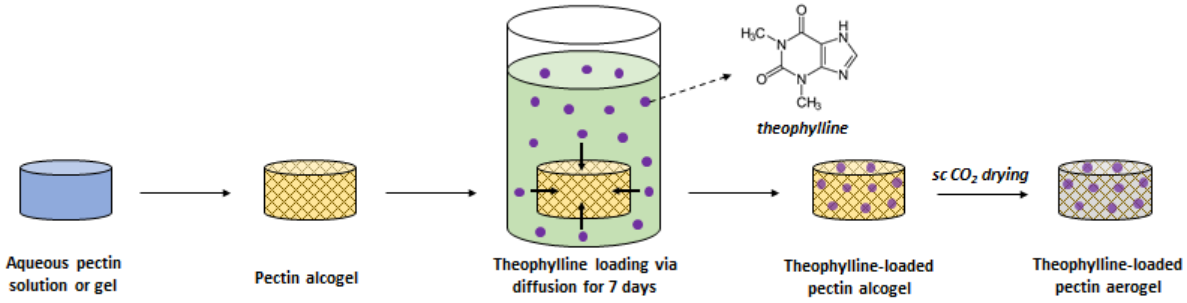

Figure 1.

Schematic illustration of the preparation of theophylline-loaded pectin aerogels.

In order to perform drying with sc CO_2, water has to be replaced by a fluid which is miscible with CO_2; ethanol was used for this purpose (it is a pectin non-solvent). Solvent exchange was performed as reported previously [27, 28] by progressively decreasing the water/ethanol (v/v) ratio to 50/50, 25/75 and 0/100, followed by final extensive washing with pure non-solvent. The resulting samples were 3D networks composed of coagulated pectin with ethanol in the pores, so-called "alcogels".

Theophylline is well soluble in water (8.3 g/L at 25°C) [29], moderately soluble in ethanol (maximal concentration 3.5 g/L at 25 °C) and insoluble in non-polar solvents such as supercritical CO_2 [30]. To avoid washing out the theophylline during solvent exchange steps, pectin alcogels were impregnated with theophylline just before drying as follows. The alcogels were immersed in theophylline-ethanol solution with a volume 25 to 30 times larger than the volume of pectin (Figure 1). The theophylline solution was renewed after 48 h and samples were immersed for 7 days in total to ensure complete drug diffusion through the sample. This duration was calculated by estimating the time needed by theophylline molecule to diffuse through a gel disk with half thickness of maximum of 5 mm. The theophylline-impregnated pectin alcogels were then dried with sc CO_2. The system was pressurized at 50 bar and 37 °C with gaseous CO_2 while the

nonsolvent was slowly drained. Afterwards, the pressure in the autoclave was increased to 80 bar to be above the CO_2 critical point. The sc CO_2 solubilized the residual nonsolvent inside the samples' pores. A dynamic washing step was then performed at 80 bar and 37 °C, at an output of 5 kg of CO_2/h for 1 h. It was followed by a static mode of 1−2 h at the same pressure and temperature and then by dynamic washing again for 2 h. Finally, the system was slowly depressurized at 4 bar/h and 37 °C, and cooled to room temperature before being opened.

2.2.2 Characterization methods

Aerogel bulk density (ρ_{bulk}) was determined as the ratio of sample mass to sample volume. The mass of the aerogel was measured with a high precision digital analytical balance. The volume was measured with a digital caliper. The errors were ± 10%.

The specific surface area S_{BET} was measured with a Micromeritics ASAP 2020 instrument using nitrogen adsorption and the Brunauer–Emmett–Teller (BET) method. The samples were degassed under high vacuum at 70 °C for 10 h prior to the measurements. The maximal standard deviation was ± 20 m^2/g.

The morphology of aerogels was studied using a Zeiss Supra 40 scanning electron microscope (SEM) equipped with a field emission gun. A layer of 7 nm of platinum was sputtered using a Q150T Quarum metallizer.

Theophylline release experiments were performed at 37 °C under sink conditions (900 ml release medium) with stirring at 100 rpm to ensure homogenization. The aerogel (disk-shaped, diameter around 2 cm, thickness around 0.8 cm) was placed in a permeable stainless-steel basket. In order to mimic the physiological conditions in the gastro-intestinal tract, aerogel was immersed first in SGF (pH 1.0) during 1 h and subsequently transferred to SIF (pH 6.8). Drug release was followed via periodical spectrophotometric measurements at a wavelength of 271 nm [31] using a

quartz cuvette with an optical path length of 10 mm. The absorption spectrum of theophylline is presented in Figure S1 of the Supporting Information. An automated set-up was used, consisting of a UV-1800 UV/Visible Scanning Spectrophotometer coupled to a 206-23790-91 Peristaltic Sipper Pump and a 160C Sipper Unit (all from Shimadzu). Calibration curves were constructed using SIF and SGF theophylline solutions of known concentrations (Figure S2).

If pectin was not completely dissolved after the release curve reached a stable absorbance plateau for more than 30 minutes, indicating that no more drug was released, the presence of theophylline in the remaining matrix was tested. The sample was crushed with a mortar and pestle, sonicated in SIF for 30 min, liquid probe taken, filtered and absorbance measured. In all cases no theophylline remained in non-dissolved matrices, and thus the actual drug dose (or the actual drug concentration) in the aerogel after the loading process was the one obtained at the absorbance plateau.

Theoretical drug dose, drug loading efficiency and aerogel loading capacity were calculated as follows:

$$Theoretical\ drug\ dose = V_{pectin}\ (cm^3) \times C_{theophylline\ in\ solution}(g.cm^{-3}) \quad (2)$$

$$Drug\ loading\ efficiency\ (\%) = \frac{actual\ drug\ dose\ (g)}{theoretical\ drug\ dose(g)} \times 100\% \quad (3)$$

$$Aerogel\ loading\ capacity\ (\%) = \frac{actual\ drug\ dose\ (g)}{aerogel\ weight\ (g)} \times\ 100\% \quad (4)$$

where V_{pectin} is the volume of the pectin alcogel in the impregnation bath containing an ethanolic theophylline solution with a theophylline concentration of $C_{theophylline\ in\ solution}$ (Figure 1).

3. Results and Discussion

It is well established that density, porosity and S_{BET} of pectin aerogels are controlled by the preparation conditions such as pectin concentration, solution pH and concentration of calcium as well as the state of the matter before solvent exchange (solution or gel) [27, 28, 32]. When the pH of a pectin solution is below pK (3 – 3.5) or calcium salt is added, the solution is gelling. When a non-solvent (ethanol) is added to a gel, it is shrinking much less than a non-gelled solution of the same pectin concentration, resulting in aerogels with lower density, larger pores and lower specific surface area [27, 28]. Figure S3 of the Supporting Information shows the main characteristics obtained previously for neat pectin aerogels as a function of solution pH and calcium concentration.

In the present work those results are used to tune and analyse the kinetics of theophylline release. Pectin concentration, solution pH and concentration of calcium were varied (one parameter varied and the others constant). To understand how aerogel properties affect the release of theophylline, first their influence on loading efficiency (eq.3) and loading capacity (eq.4) was analyzed. Then an example of pectin volume, mass and theophylline release evolution in time is shown and the applicability of the existing drug release kinetics models for the case of theophylline release from pectin aerogel is tested. Finally, the influence of pectin solution pH and calcium concentration on release kinetics is investigated.

3.1 Influence of pectin aerogel characteristics on theophylline loading efficiency and loading capacity

The influence of the density and specific surface area of theophylline-loaded pectin aerogel on the loading efficiency is presented in Figure 2a and b, respectively. All data, i.e. from 3% and 6% pectin solutions at different pH and calcium concentrations, are put together. Loading efficiency varies from 40% to 80% correlating well with the values known from literature for other bio-aerogels being usually from 15% to 80% [19, 20, 26, 33].

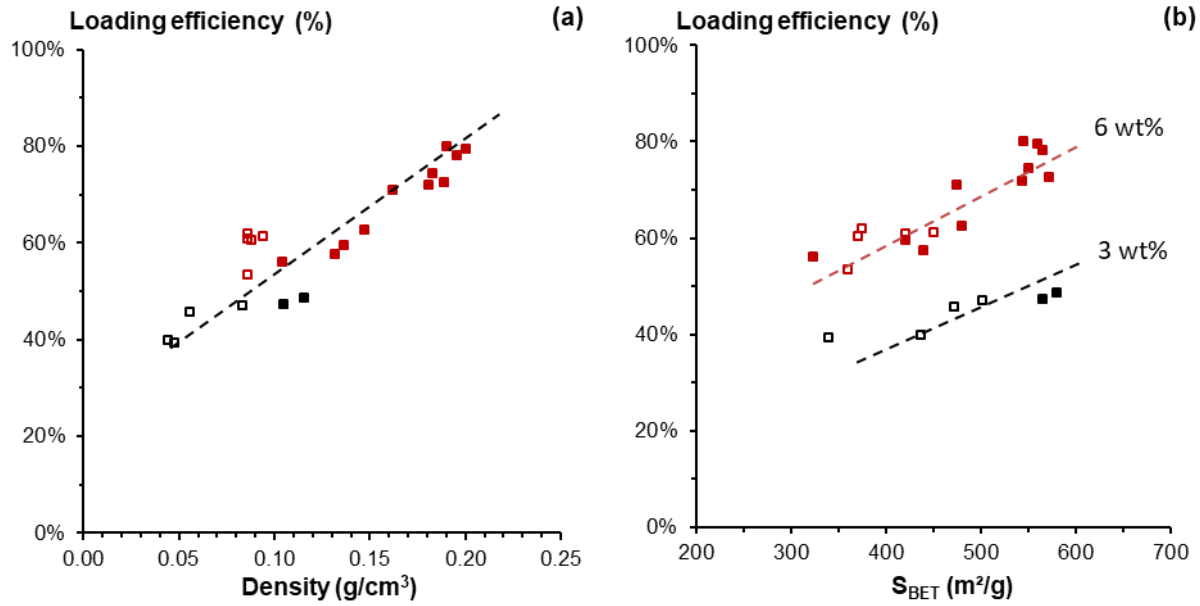

Figure 2.

Loading efficiency as a function of aerogel density (a) and specific surface area (b) for pectin aerogels made from pectin solutions of either 3 wt% (black squares) or 6 wt% (red squares), in the absence of calcium at different pH (filled symbols) or crosslinked with calcium at different R(Ca) (open symbols). Theophylline concentration in the impregnation baths was 2.5 or 3.4 g/L. Dashed line is given to guide the eye.

Despite that theophylline is not soluble in CO_2, the loading efficiency is below 100%. Two reasons can be given: i) incomplete impregnation of theophylline in pectin alcogel and ii) washing out of theophylline during sc drying. The first reason can be excluded as the concentration of theophylline was measured in loaded alcogels but dried in vacuum and crash test was used as described in the Experimental section; the loading efficiency was 95-100%. This confirmed that diffusion time during the impregnation was sufficient for theophylline to penetrate the alcogel to the core. It should also be noted that the radius of a theophylline molecule is around 3.5 – 4 nm

[34, 35]; it is significantly smaller than aerogel pores' dimensions, as it will be shown below, thus excluding steric hindrance for drug penetration inside the pectin network. The second reason remains: it is hypothesized that because of the miscibility of ethanol and CO_2, a certain portion of the drug is washed out due to CO_2 circulation and mixing with ethanol at the beginning of sc drying.

Loading efficiency increases with the increase of aerogel bulk density (Figure 2a); the highest values, up to 70-80%, are achieved for aerogels with the highest density ($0.16 < \rho_{bulk} < 0.20$ g/cm^3). Higher density is reflected by aerogel morphology, as shown in Figure 3 for aerogels made from 6% solutions at different solution pH. Bringing the pH below the pKa of pectin (~ 3.0 - 3.5) results in decreased ionization of galacturonic acid groups which in turn reduces coulombic repulsions and promotes chain aggregation due to hydrogen bonding and hydrophobic interactions. Therefore, at lower pH values solutions are gelling opposite to solutions at pH 2 and 3. The increase of pectin solution pH from 1.2 to 3 almost doubles aerogel density and results in a strong decrease of pore size. Denser the network, smaller the pores with higher tortuosity thus better preventing theophylline wash out during sc drying process. Lower the solution pH, stronger the gels, less they shrink during solvent exchange resulting in lower density and larger pores [27]. Lower loading efficiency was also obtained for the gelling pectin solution when crosslinked with calcium (Figure 2a): higher the calcium concentration, lower the shrinkage and thus lower the density and larger the pores, as demonstrated in Figure 4 for aerogels from pectin solutions of 3 % crosslinked with calcium of various concentrations.

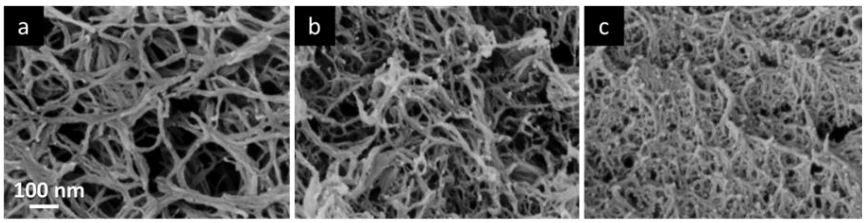

State of the matter before solvent exchange	gel	solution	solution
Bulk density (g/cm^3)	0.105	0.136	0.181
S_{BET} (m^2/g)	323	421	544

Figure 3.

Network morphologies observed by SEM, density and specific surface area of theophylline-loaded pectin aerogels prepared from 6 wt% pectin dissolved at pH 1.2 (a), pH 2.0 (b) and pH 3.0 (c) in the absence of calcium. The scale is the same for all images.

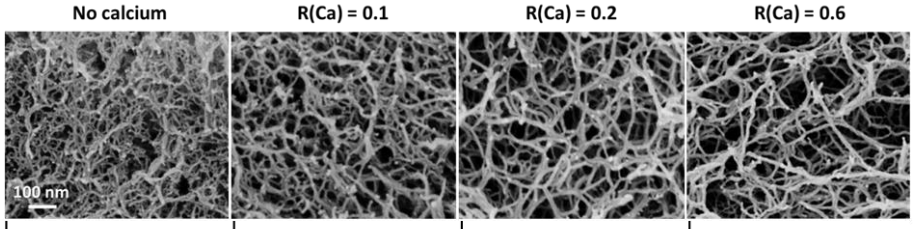

State of the matter before solvent exchange	solution	gel	gel	gel
Bulk density (g/cm^3)	0.118	0.085	0.056	0.044
S_{BET} (m^2/g)	574	502	472	437

Figure 4.

Network morphologies observed by SEM, density and specific surface area of theophylline-loaded pectin aerogels prepared from 3% solutions at pH 3.0 with increasing calcium ratio R(Ca) from 0 to 0.6.

Figure 2b shows that the drug loading efficiency also increases with aerogel specific surface area. An offset is visible between the 6% and 3% samples as practically all 6% aerogels have a higher density than all 3% aerogels (see Figure 2a). Literature suggests that the direct correlation between the loading efficiency and specific surface area is due to the amount of internal pores' surface available for drug deposition [24, 33, 36-38]. This may be true when pores' surface is functionalized to bind the drug. However, in our view this interpretation can be misleading in the case of no interactions between the aerogel and drug molecule. Indeed, ~ 100% loading efficiency was obtained for different pectin formulations but when alcogels were dried in vacuum which is the sign that specific surface area is not directly responsible for drug deposition. It was recently shown by our group that theophylline release from pectin xerogels takes several hours [39], excluding the possibility that drug remained near the surface during loading, where it would have dissolved very rapidly. In the case of pectin alcogel loaded with theophylline there are no physical or chemical interactions between the polymer and the drug. Two observations confirm this hypothesis: (1) the drug is completely released from the aerogels, even from non-fully dissolved networks; and (2) the drug is partly washed out from the pectin networks during $scCO_2$ drying. It is hypothesized that it is the higher network tortuosity, which accompanies a higher specific surface area, that prevents theophylline washout during $scCO_2$ drying, resulting in a higher loading efficiency.

Theophylline loading capacity as a function of aerogel density and specific surface area is shown in Figures 5a and b, respectively. It increases with specific surface area and does not show any trend as a function of aerogel density. Loading capacity is considerably lower (from 2 to 4.5 %) than that reported for other drugs loaded in bio-aerogels in other works (~15 - 80 %) [19, 20, 23, 24, 26]. The reason is that in those studies other impregnation methods were employed. The loading capacity strongly depends on the drug solubility in the loading medium, and thus on the drug

concentration in the impregnation solvent relative to the mass of the carrier. For example, if using hydrophobic drugs soluble in CO_2 impregnated in pectin matrix at the last step of supercritical drying, the loading capacity is much higher. The low drug loading capacities obtained in this study are the result of the moderate solubility of theophylline in ethanol (maximum 3.5 g/L at 25 °C) and the relatively high concentrations of the pectin solutions (up to 6 wt%) to produce the pectin aerogels. The low drug content may explain why no theophylline is seen on SEM images of the internal structure of theophylline-loaded pectin aerogels (Figures 3 and 4), and why the structural and physical properties of theophylline-loaded pectin aerogels are the same as the neat counterparts (Figure S3d).

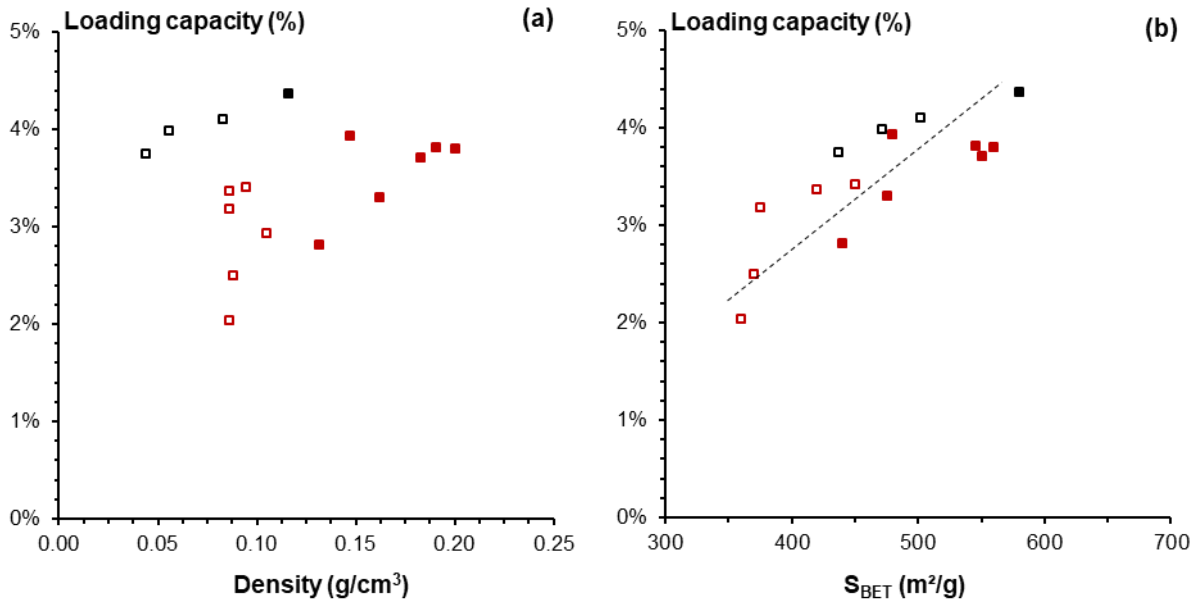

Figure 5

Loading capacity as a function of aerogel density (a) and specific surface area (b) for pectin aerogels made from pectin solutions of either 3 wt% (black squares) or 6 wt% (red squares), in the absence of calcium at different pH (filled symbols) or crosslinked with calcium at different R(Ca) (open symbols). Dashed line is given to guide the eye.

3.2. Overall description of pectin aerogel evolution in SGF and SIF media and theophylline release

To mimic the physiological conditions for oral administration, theophylline-loaded pectin aerogels were first immersed in SGF (pH 1.0) for 1 hour and subsequently in SIF (pH 6.8). The example of cumulative drug release, matrix mass and volume evolution over time (Figure 6) for pectin aerogels prepared at pH 3.0 without calcium are discussed in detail below. Examples of release results' reproducibility are shown in Figure S4. Release rates (Figure 6d) were estimated by calculation of the slopes from the theophylline release curve (Figure 6a) considering a linear function between two points separated by 5 or 10 minutes.

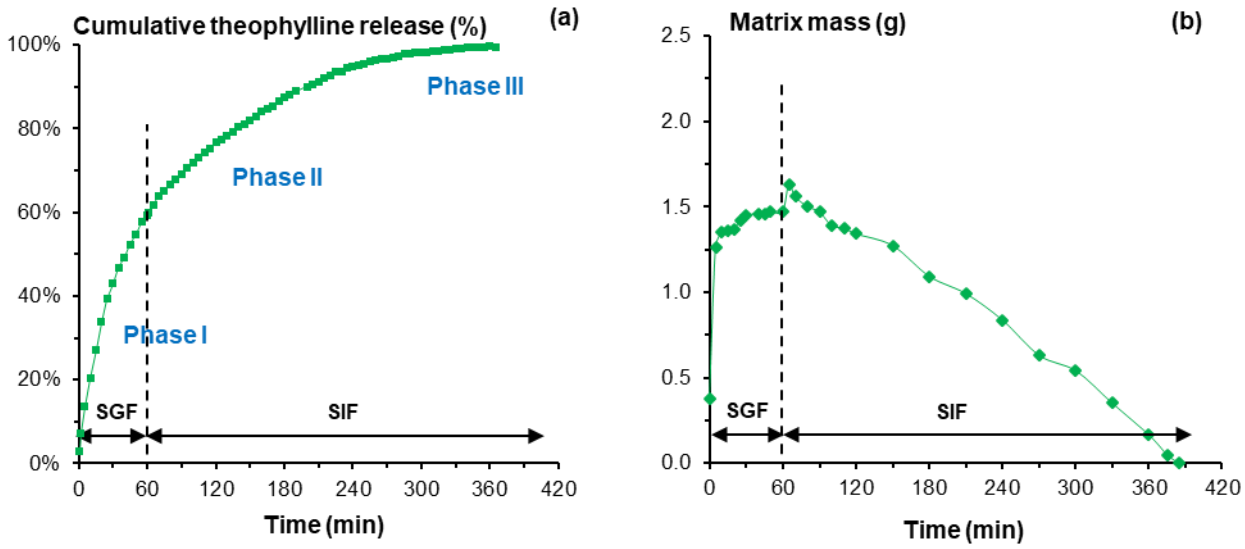

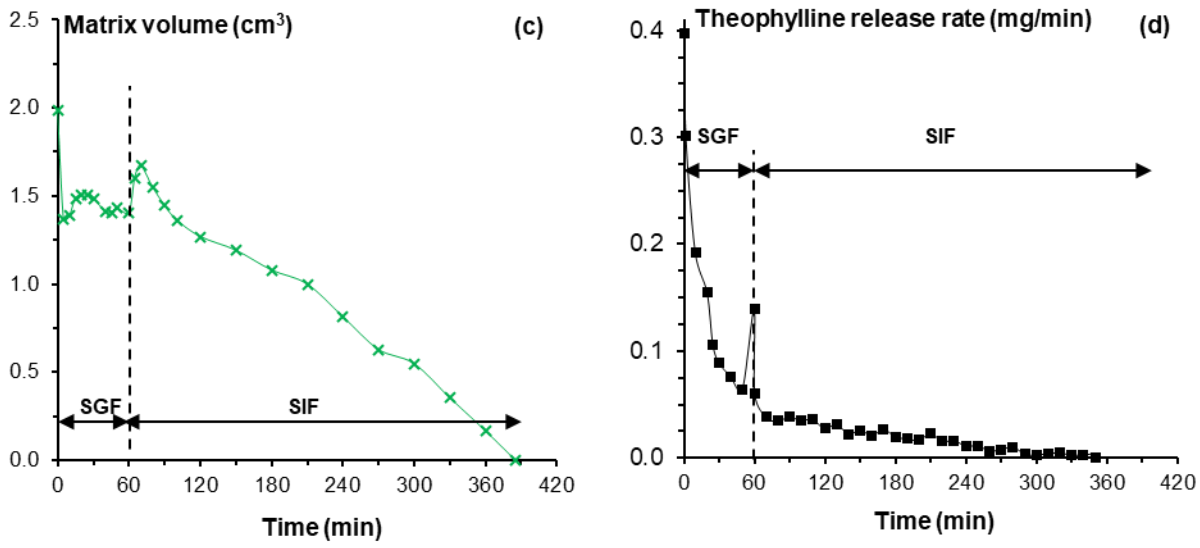

Figure 6.

Example of cumulative theophylline release (a), matrix mass (b), volume (c) and rate of release (d) as a function of time for pectin aerogels prepared from 6 wt% pectin dissolved at pH 3.0 in the absence of calcium. In this example, 14.2 mg of theophylline was loaded in 360 mg of pectin aerogel. Lines are given to guide the eye.

During the first 10 minutes of immersion in release medium (SGF, pH 1.0), the pectin aerogels exhibit a fast mass increase due to water uptake (Figure 6b). The initial volume shrinkage may be due to the collapse of pores because of capillary forces exerted by the fast water penetration into the system (Figure 6c) [40]. The release medium is of low pH; the hydrogen bonding between pectin chains are promoted preventing matrix swelling and dissolution. During the next 50 min pectin chains are hydrated resulting in the formation of a gel layer surrounding the dry core (Figure S5). These results confirm that pectin aerogels are gastro-resistant materials that can be used to protect drugs from gastric degradation and to prevent full drug release in the stomach.

Upon change of the release medium from SGF to SIF (pH 6.8), ionization of the carboxylate groups of pectin occurs, and pectin chains repel each other due to coulombic repulsion. As a result, the highly hydrated chains disentangle and start to dissolve as revealed by strong matrix swelling followed by dramatic erosion until full dissolution (here, after 390 min) (Figures 6b and 6c). The matrix mass and volume evolution over time can be used to explain the kinetics of theophylline release from the pectin aerogel (Figure 6a), for which different phases can be distinguished.

Phase I: After immersion of the aerogel in the release medium, the drug that is located on and near the surface immediately dissolves due to the high solubility of theophylline in aqueous media. It leads to a typical fast initial release, during which a high quantity of drug is released in a short period of time (Figure 6a). It is characterized by the highest theophylline release rate (Figure 6d, ~0.11 - 0.40 mg theophylline/min, corresponding to ~ 1.1 - 2.8 wt%/min of the total theophylline content). For the aerogel featured in Figure 6, approximately 20% of the total amount of theophylline is released in the first 10 minutes of the experiment. The release of the accessible fraction of drug close to the surface is governed by Fickian diffusion, as the chemical gradient is the only driving force: the drug located near the surface is freely accessible, and the impact of polymer relaxation is considered to be negligible. A fast initial release may be either pharmacologically undesirable and economically inefficient, or, in certain situations, a rapid release quickly achieving the therapeutic efficiency range may be advantageous [41].

The first phase is ending by a lag time before the matrix erosion phase starts in SIF. For drug molecules that are located deeper in the matrix, the time to diffuse out of the matrix becomes longer. At the interface of the matrix and the solvent a viscous pectin gel layer is formed (Figure S5) which acts as a physical barrier that limits mass transport of both drug and solvent. In SGF media the chains are linked by hydrogen and hydrophobic interactions as a result of the low pH. As the diffusion times of both the solvent and theophylline become longer, the release of theophylline

over time slows down. It is characterized by lower theophylline release rates between 0.06 and 0.11 mg/min (Figure 6d, ~ 0.5 to 0.8 wt%/min of the total theophylline content). In parallel, the impact of chain relaxation on the release becomes significant as the remaining drug is less accessible and requires polymer swelling and dissolution to diffuse out of the matrix.

Phase II: After the first hour, SGF is changed for SIF. Higher pH promotes ionization of pectin chains, solvent penetration into the aerogel is promoted and the matrix instantly swells (Figure 6c) resulting in a sharp increase in release rate observed at t = 60 min (Figure 6d). The pectin aerogel subsequently dissolves, which in turn facilitates solvent and drug diffusion. This phase corresponds to the period of approximately 60 - 95 % of the cumulated drug release and concerns the drug that was not freely accessible. During Phase II, progressive pectin chain relaxation, re-arrangement, swelling and dissolution occur, which significantly impact the release kinetics. Erosion-controlled release begins as the aerogel matrix progressively dissolves, starting at the erosion front on the outer surface. The erosion front gradually moves inward, as shown by the decrease in mass and volume of the aerogel (Figures 6b and 6c). Thus, after the fast initial release phase (Phase I) and a lag time, during Phase II the different mass transport phenomena eventually are equilibrated leading to nearly steady-state release that lasts the major part of the release. Theophylline is then released at rates between 0.02 and 0.04 mg/min (Figure 6d, ~ 0.11 - 0.25 wt%/min of the total theophylline content). This nearly steady-state release is appealing for pharmaceutical applications as it delivers a constant dose over a prolonged period of time.

Phase III: The final stage of the release is characterized by a very low release rate (Figure 6d, 0.003-0.010 mg/min, ~ 0.02- 0.07 wt%/min of the total theophylline content) as the drug inside the matrix runs out. Full theophylline release occurs just before the pectin aerogel matrix completely dissolves (Figure 6b, c).

Tests on the release kinetics separately in SGF and in SIF at 37 °C were also performed. Figure S6 shows the cumulative theophylline release from pectin aerogels (6 wt% pectin dissolved at pH 3.0 in the absence of calcium) over time in either SGF medium or in SIF medium. These control experiments confirm that complete theophylline release is much faster in SIF (265 min) than in SGF (1050 min), as observed under model physiological conditions in the gastro-intestinal tract (Figure 6a). The observed slow drug release in SGF and fast drug release in SIF, caused in part by the respective stability and instability of pectin in these media, is in accordance with previous literature [19, 23, 25, 26].

3.3. Selection of drug release kinetic models to describe the release of theophylline from pectin aerogels

Bio-aerogels are nanostructured dry highly porous networks, and it is hypothesized that they combine the properties of a polymer gel and of a dry polymer matrix of high porosity and interconnected pores. The following models are known to describe drug release from a solid polymer matrix (Table S1): Higuchi, Korsmeyer-Peppas, Peppas-Sahlin, Hixson-Crowell, Hopfenberg and Gallagher-Corrigan [42]. The goal here is to select the model(s) to use for the following analysis of two case studies: the influence of pectin solution pH and of calcium concentration, on theophylline release. Zero-order kinetics are not considered as theophylline release rates over time were different. The first-order model is also not considered as it does not take into account polymer relaxation and dissolution.

The Higuchi model (Table S1) is used to describe drug release based on Fickian diffusion of both the solvent and the drug. This model assumes that dissolution and/or swelling of the matrix are negligible. The experimental data in Figure 6a were approximated with the Higuchi model (not shown) and the correlation coefficient R^2 was $0.8 < R^2 < 0.9$. The reason of rather low R^2 is that as

shown in Figure 6b, c, pectin aerogel matrix is soluble in SIF medium, and pectin chain relaxation, matrix swelling and erosion are expected to impact the drug release. This model will thus not be used in the following.

Both Hopfenberg and Hixson-Crowell models are applicable when drug release is controlled by the dissolution rate of the matrix (erosion). This is the case when pectin aerogel is in SIF but not the first hour in SGF (Figure 6b, c). The correlation coefficients with experimental data (not shown) were rather high, $0.95 > R^2 > 0.99$, but these models will not be used in the following as they do not reflect the release mechanism for the first hour and also other models were found to better fit experimental data, as shown below.

Peppas models [43, 44] consider diffusion and relaxation mechanisms. The *n* value of 0.58 was obtained after fitting the experimental data from Figure 6a for the first 60 % of drug release with Korsmeyer–Peppas model (Table S1 and Figure S7), with $R^2 > 0.99$. This *n* value is characteristic for an anomalous transport indicating that both solvent diffusion and polymer relaxation must be considered, which is in line with the experimental data shown in Figure 6 during Phase I, which includes a fast initial release and a lag time.

Peppas-Sahlin model (Table S1) can be used to estimate the contribution of diffusion vs relaxation mechanism. The results presented in Figure S8 for the first 60% of release show that the diffusional mechanism decreases with time: in SGF medium pectin chains are protonated and not dissolving within the first hour (matrix mass and volume do not change, see Figure 6b, c).

The Gallagher-Corrigan model describes a two-step drug release profile (anomalous transport), starting with an initial burst phase and followed by a slower matrix erosion-governed controlled release (Table S1). Figure S9a shows the fit to experimental data from Figure 6a. The important contribution of matrix erosion to the drug release in SIF (Phase II) follows not only from experimental observations (Figure 6c), but also from the high erosion kinetic constant $k_e \sim 3.1\ h^{-1}$

as compared to the burst constant $k_b \sim 0.1\ h^{-1}$ (Figure S9b). The reason is that in SIF pectin chains become ionized and dissolve. As shown for the example of release in Figure 6 and for the case studies described below, the Gallagher-Corrigan model provides the best fit to all our experimental data. A similar observation was reported for ketoprofen release from pectin and alginate aerogels in SIF alone and in SGF alone [20]. However, one should keep in mind that the beginning of release, despite being fast, is not an abrupt burst as assumed by the Gallagher-Corrigan model.

Concluding, theophylline release from pectin aerogels in the first hour in SGF medium and then in SIF medium is governed by fast initial drug dissolution, diffusion through hydrated aerogel pores followed by relaxation and erosion mechanisms, corresponding to complex anomalous (non-Fickian) transport. In the following, the Peppas-Sahlin model will be used to estimate the input of the diffusional mechanism up to 60% of the released drug and the Gallagher-Corrigan model to analyze the entire release period.

3.4. Influence of pectin solution pH on theophylline release kinetics from pectin aerogel

Figure 7 shows how the pH of the starting pectin solutions, and as a consequence, different structural properties of pectin aerogels, impact the drug release properties. Pectin aerogels prepared from solutions at lower pH (lower aerogel density, see Figure 3) are faster drug delivery systems, with a complete theophylline release in 250 min, 290 and 350 min for aerogels prepared at pH 1.2, 2.0 and 3.0, respectively. The low-density network obtained from gelled pectin solutions at low pH (Figure 3) facilitates water penetration in the system and its larger free volume increases solvent and drug diffusivity and promotes matrix dissolution (Figure 8). The faster release is correlated with faster matrix erosion/dissolution (Figures 7b, c). In contrast, denser aerogel network obtained from non-gelled solution at higher pH, having smaller pores, likely slows down the diffusion of solvent into the aerogels, which in turn slows down matrix dissolution and thus the release of

theophylline. Similar to aerogels prepared at pH 3.0 (*vide supra*), the beginning of release from aerogels prepared at pH 1.2 and 2.0 is due to anomalous transport, as revealed by *n* exponent values between 0.45 and 0.89 using the Korsmeyer-Peppas model.

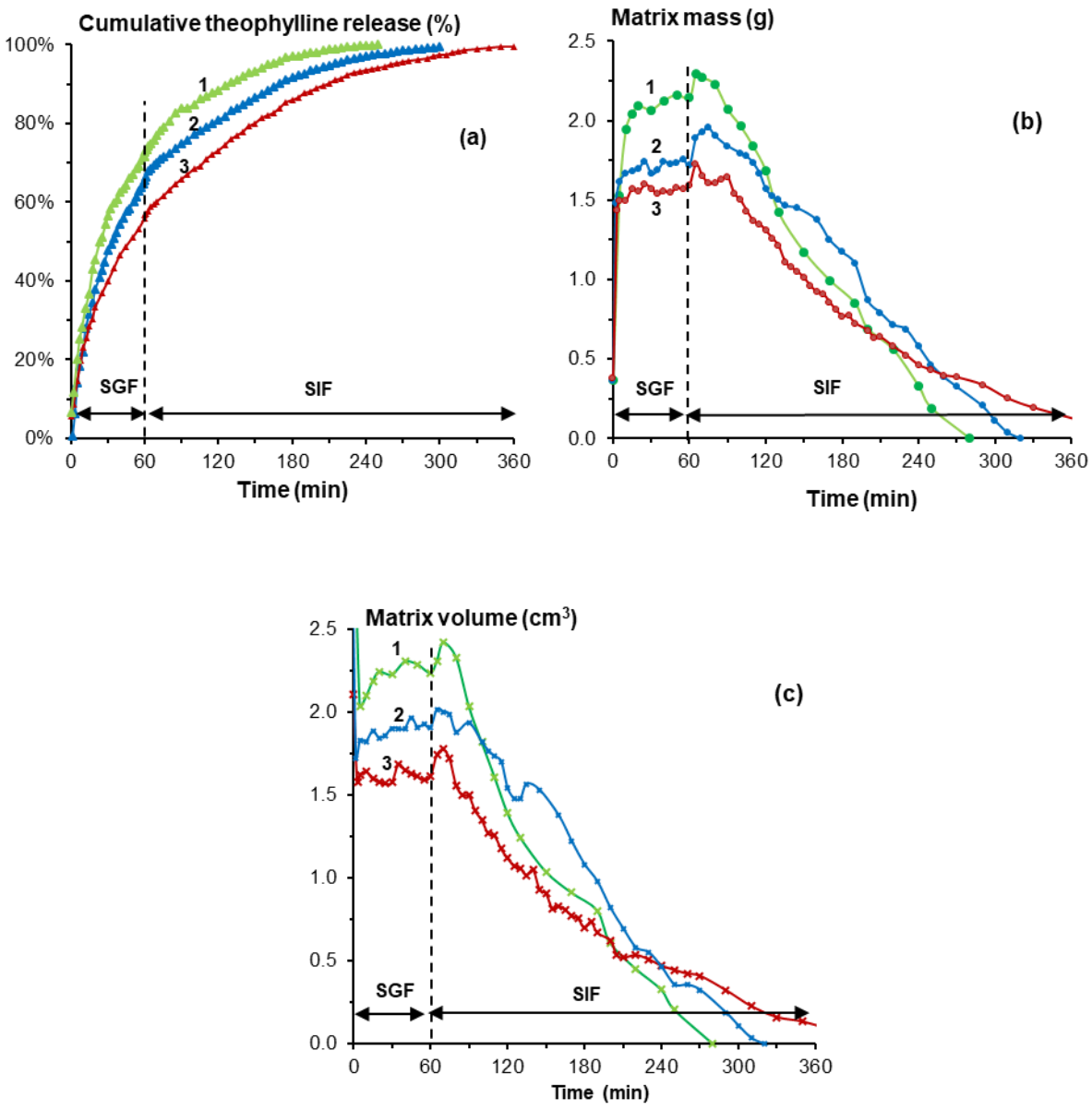

Figure 7.

Example of cumulative theophylline release (a), matrix mass (b) and matrix volume (c) over time for pectin aerogels prepared from 6 wt% pectin dissolved at pH 1.2 (1), 2.0 (2) or 3.0 (3) in the absence of calcium; theophylline concentration in the impregnation solution was 2.5 g/L. Lines are given to guide the eye.

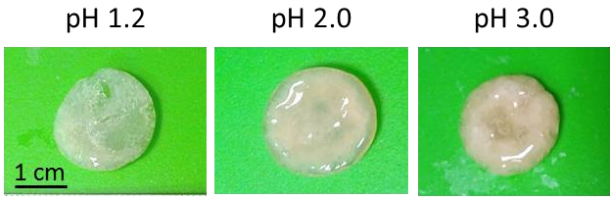

Figure 8.

Pictures of theophylline-loaded pectin aerogels during release at t = 180 minutes. The samples are the same as in Figure 7.

The plot of the Fickian release contribution obtained from the Peppas-Sahlin model (Figure S10, which contains recalculated experimental data from Figure 7a) shows that the lower the aerogel density, the quicker is the decrease of the Fickian mechanism contribution. In addition, it follows from Figure S11 that the burst constant k_b in the Gallagher-Corrigan model slightly increases from 0.10 h^{-1} to 0.13 h^{-1}, while the erosion constant k_e clearly increases from 3.01 h^{-1} to 4.61 h^{-1} with the decrease of aerogel density (pectin solution pH decreases from 3.0 to 1.2). This confirms that the diffusion rate at the beginning as well as the matrix erosion rate are higher due to the lower density obtained at lower pH.

3.5. Influence of calcium concentration on theophylline release kinetics from pectin aerogel

The influence of calcium crosslinking on the release behavior of theophylline was investigated as well (Figure 9). Figure 9a shows that the presence of calcium slows down theophylline release from the aerogels, despite the lower network density and the presence of larger pores (Figure 4). The slower release is likely due to the intermolecular ionic crosslinks which make the network more "resistant" to polymer dissolution and matrix erosion (Figures 9b, c and 10). The plot of the Fickian release fraction over time (Figure S12), as determined from the Peppas-Sahlin model, illustrates the increasing contribution of diffusion and decreasing contribution of erosion as R(Ca) increases. Moreover, the Fickian coefficient K_F increases and the relaxational coefficient K_R decreases upon R(Ca) increase (Figure S12). Fitting the experimental data in the Gallagher-Corrigan model yields similar results as the erosion constant k_e decreases upon R(Ca) increase (Figure S13).

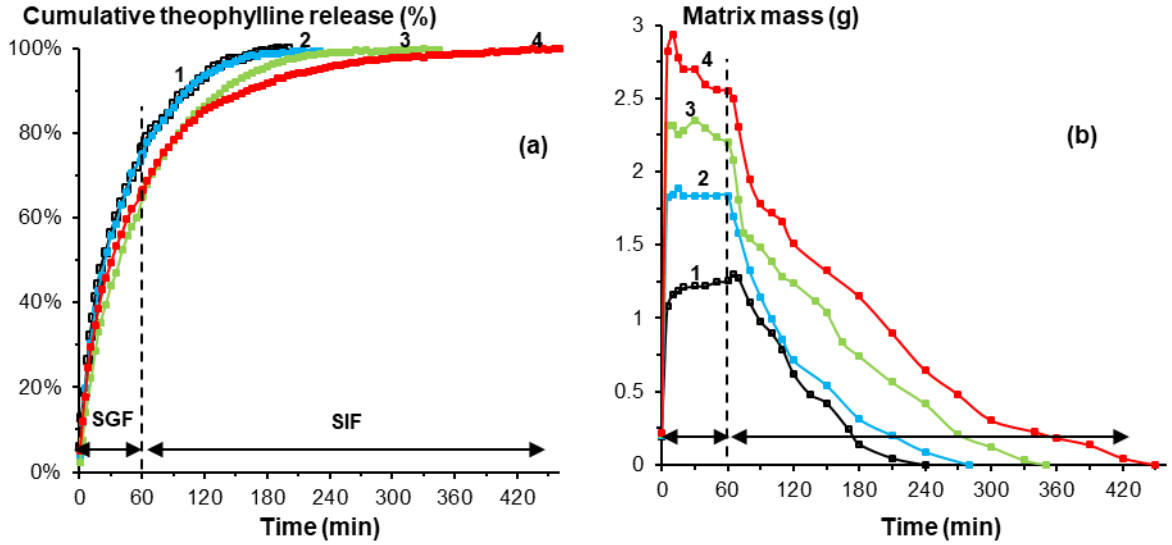

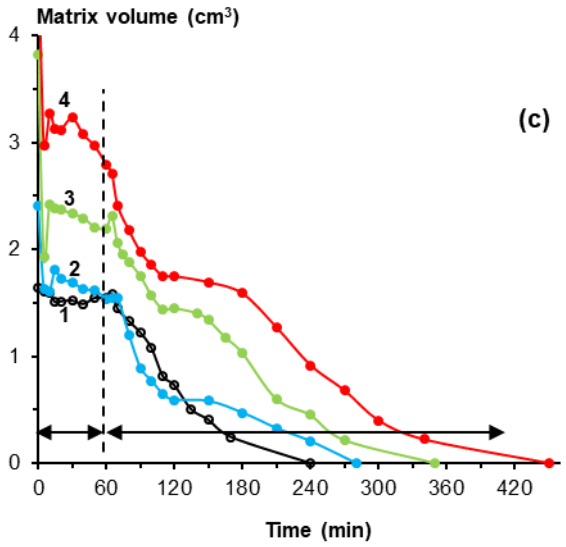

Figure 9.

Cumulative theophylline release (a), matrix mass (b) and matrix volume (c) over time for pectin aerogels prepared from 3 wt% pectin dissolved at pH 3.0 with increasing calcium ratio R(Ca): 0 (1), 0.1 (2), 0.2 (3) and 0.6 (4); theophylline concentration in the impregnation solution was 3.4 g/L. Lines are given to guide the eye.

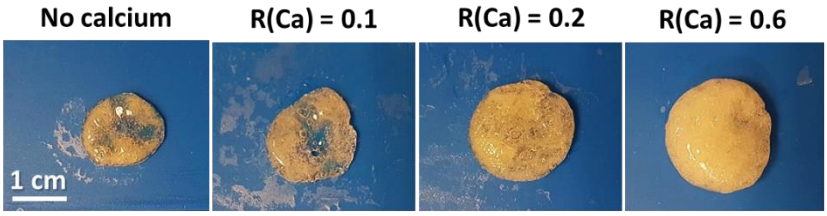

Figure 10.

Pictures of theophylline-loaded pectin aerogels during release at t = 180 minutes. The samples are the same as in Figure 9.

3.6. Influence of density and specific surface area on the total release time

The influence of aerogel density and specific surface area on the total time of theophylline release is summarized in Figure 11a and 11b, respectively, for all studied aerogels. For the non-crosslinked pectin, higher density and specific surface area induce a longer release time, as described in Section 3.4. This is an expected result: higher density and smaller pores slow down drug diffusion out of the matrix.

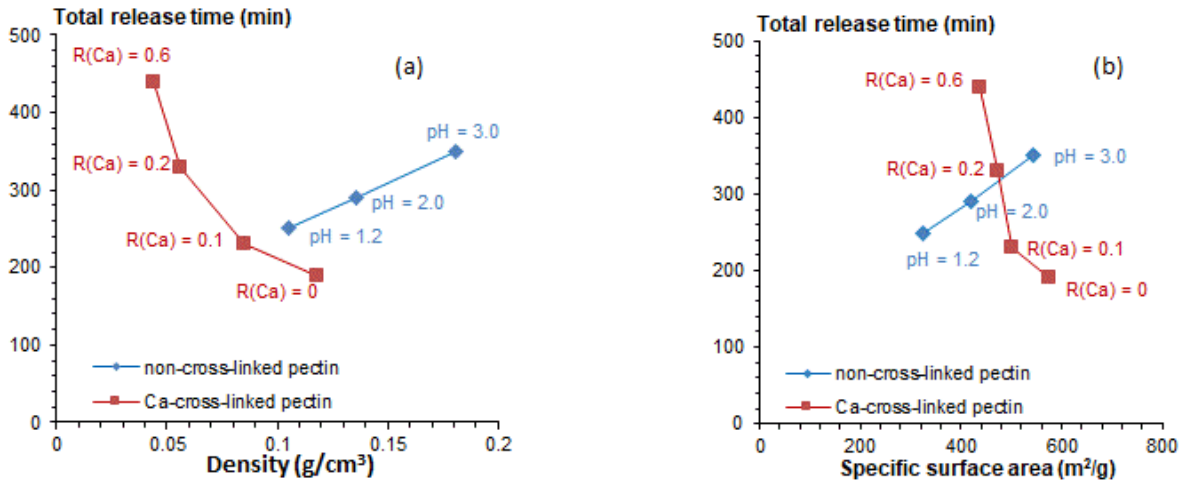

Figure 11.

Total release time as a function pectin aerogel density (a) and specific surface area (b) Non-crosslinked pectin was from 6 wt% solution at various pH (as in Figure 7) and calcium crosslinked from 3 wt% pectin dissolved at pH 3.0 with increasing calcium ratio R(Ca) from 0 to 0.6 (as in Figure 9). The variation in total release time for a given pectin aerogel formulation was found to be 15 minutes at most. Lines are given to guide the eye.

On the opposite, the higher density and surface area of calcium crosslinked pectin aerogels lead to a quicker release. This surprising from the first glance result is explained by pectin solubility which is decreased with the increase of calcium concentration. It turned out that the effect of the increased “resistance” against matrix erosion upon R(Ca) increase is dominating the effect of the

lower network density and larger pores. While the release during the first hour in SGF is governed by the anomalous diffusion for all pectin aerogels, the release in SIF is controlled by matrix erosion and dissolution and thus crosslinking starts to play the major role.

4. Conclusions

In this study, structural and physico-chemical properties of pectin aerogels were systematically varied by adjusting the preparation conditions and gelation mechanisms in order to establish structure-properties correlations that explain the loading and release behavior of the hydrophilic drug theophylline. The loading efficiency and loading capacity increase with aerogel specific surface area. It is hypothesized that the higher loading efficiency results from the higher network tortuosity, which accompanies a higher specific surface area and prevents theophylline washout during $scCO_2$ drying. The loading efficiency also correlates with aerogel density as denser networks have a smaller pore size which prevents theophylline washout during sc CO_2 drying.

The release of theophylline from pectin aerogels into SGF medium (first hour) and subsequently into SIF medium is governed by fast initial drug dissolution, diffusion through hydrated aerogel pores followed by relaxation and erosion mechanisms, corresponding to complex anomalous (non-Fickian) transport. A lower pH of the pectin starting solution results in a faster theophylline release because the lower density network obtained at low pH enhances solvent and drug diffusion and facilitates matrix dissolution. Calcium crosslinking decreases the theophylline release rate because the intermolecular ionic crosslinks enhance the resistance of the network against polymer dissolution and matrix erosion. This effect prevails over the influence of the lower network density and larger pores upon calcium crosslinking.

Our observations regarding the main release mechanism and its dependence on the preparation conditions were corroborated by the Peppas-Sahlin model, which was selected to determine the

input of the diffusional mechanism up to 60% of release, as well as the Gallagher-Corrigan model, which was used to analyze the complete release period. In summary, this study demonstrates how pectin aerogel properties can be controlled by tuning pectin initial solution pH and calcium concentration in order to obtain desired release kinetics. In a broader perspective, the obtained knowledge can be extended to the release kinetics of hydrophilic drugs from other bio-aerogels based on polyelectrolyte polysaccharides such as alginate and carrageenan.

Acknowledgements

We thank Cargill, France, for providing pectin, Pierre Ilbizian (PERSEE, Mines ParisTech, France) for supercritical drying, Laurent Schiatti De Monza (PERSEE, Mines ParisTech, France) for setting the automatic recording of theophylline release and Suzanne Jacomet (CEMEF, Mines ParisTech) for help with SEM imaging.

Funding

This research did not receive any specific grant from funding agencies in the public, commercial, or not-for-profit sectors.

References

[1] K. Ganesan, T. Budtova, L. Ratke, P. Gurikov, V. Baudron, I. Preibisch, P. Niemeyer, I. Smirnova, B. Milow, Review on the production of polysaccharide aerogel particles, Materials 11 (2018) 2144.

[2] N. Lavoine, L. Bergström, Nanocellulose-based foams and aerogels: processing, properties, and applications, J. Mater. Chem. A. 5 (2017) 16105-16117.

[3] T. Budtova, Cellulose II aerogels: A review, Cellulose 26 (2019) 81-121.

[4] S. Zhao, W.J. Malfait, N. Guerrero-Alburquerque, M.M. Koebel, G. Nyström, Biopolymer aerogels and foams: Chemistry, properties, and applications, Angew. Chem., Int. Ed. 57 (2018) 7580-7608.

[5] F. Quignard, R. Valentin, F. Di Renzo, Aerogel materials from marine polysaccharides, New J. Chem. 32 (2008) 1300-1310.

[6] T. Budtova, D.A. Aguilera, S. Beluns, L. Berglund, C. Chartier, E. Espinosa, S. Gaidukovs, A. Klimek-Kopyra, A. Kmita, D. Lachowicz, F. Liebner, O. Platnieks, A. Rodríguez, L.K. Tinoco Navarro, F. Zou, S.J. Buwalda, Biorefinery approach for aerogels, Polymers 12 (2020) 2779.

[7] T.A. Esquivel-Castro, M.C. Ibarra-Alonso, J. Oliva, A. Martínez-Luévanos, Porous aerogel and core/shell nanoparticles for controlled drug delivery: A review, Mater. Sci. Eng., C 96 (2019) 915-940.

[8] C.A. García-González, T. Budtova, L. Durães, C. Erkey, P. Del Gaudio, P. Gurikov, M. Koebel, F. Liebner, M. Neagu, I. Smirnova, An opinion paper on aerogels for biomedical and environmental applications, Molecules 24 (2019) 1815.

[9] P. Franco, I. De Marco, Supercritical CO2 adsorption of non-steroidal anti-inflammatory drugs into biopolymer aerogels, J. CO2 Util. 36 (2020) 40-53.

[10] M. Alnaief, R.M. Obaidat, M.M. Alsmadi, Preparation of hybrid alginate-chitosan aerogel as potential carriers for pulmonary drug delivery, Polymers 12 (2020) 2223.

[11] Z. Ulker, C. Erkey, An emerging platform for drug delivery: Aerogel based systems, J. Controlled Release 177 (2014) 51-63.

[12] M.P. Batista, V.S.S. Gonçalves, F.B. Gaspar, I.D. Nogueira, A.A. Matias, P. Gurikov, Novel alginate-chitosan aerogel fibres for potential wound healing applications, Int. J. Biol. Macromol. 156 (2020) 773-782.

[13] G.A. Martău, M. Mihai, D.C. Vodnar, The use of chitosan, alginate, and pectin in the biomedical and food sector - biocompatibility, bioadhesiveness, and biodegradability, Polymers 11 (2019) 1837.

[14] I. Plashchina, M. Semenova, E. Braudo, V. Tolstoguzov, Structural studies of the solutions of anionic polysaccharides. IV. Study of pectin solutions by light-scattering, Carbohydr. Polym. 5 (1985) 159-179.

[15] M.L. Fishman, P.H. Cooke, H.K. Chau, D.R. Coffin, A.T. Hotchkiss, Global structures of high methoxyl pectin from solution and in gels, Biomacromolecules 8 (2007) 573-578.

[16] D. Oakenfull, A. Scott, Hydrophobic interaction in the gelation of high methoxyl pectins, J. Food Sci. 49 (1984) 1093-1098.

[17] I. Braccini, S. Pérez, Molecular basis of Ca2+-induced gelation in alginates and pectins: the egg-box model revisited, Biomacromolecules 2 (2001) 1089-1096.

[18] F. De Cicco, P. Russo, E. Reverchon, C.A. García-González, R.P. Aquino, P. Del Gaudio, Prilling and supercritical drying: A successful duo to produce core-shell polysaccharide aerogel beads for wound healing, Carbohydr. Polym. 147 (2016) 482-489.

[19] G. Tkalec, Ž. Knez, Z. Novak, PH sensitive mesoporous materials for immediate or controlled release of NSAID, Microporous Mesoporous Mater. 224 (2016) 190-200.

[20] C.A. García-González, M. Jin, J. Gerth, C. Alvarez-Lorenzo, I. Smirnova, Polysaccharide-based aerogel microspheres for oral drug delivery, Carbohydr. Polym. 117 (2015) 797-806.

[21] V.S.S. Gonçalves, P. Gurikov, J. Poejo, A.A. Matias, S. Heinrich, C.M.M. Duarte, I. Smirnova, Alginate-based hybrid aerogel microparticles for mucosal drug delivery, Eur. J. Pharm. Biopharm. 107 (2016) 160-170.

[22] G. Horvat, K. Xhanari, M. Finšgar, L. Gradišnik, U. Maver, Ž. Knez, Z. Novak, Novel ethanol-induced pectin–xanthan aerogel coatings for orthopedic applications, Carbohydr. Polym. 166 (2017) 365-376.

[23] G. Tkalec, Ž. Knez, Z. Novak, Fast production of high-methoxyl pectin aerogels for enhancing the bioavailability of low-soluble drugs, J. Supercrit. Fluids 106 (2015) 16-22.

[24] G. Horvat, M. Pantić, Ž. Knez, Z. Novak, Encapsulation and drug release of poorly water soluble nifedipine from bio-carriers, J. Non-Cryst. Solids 481 (2018) 486-493.

[25] M. Pantic, G. Horvat, Ž. Knez, Z. Novak, Preparation and Characterization of Chitosan-Coated Pectin Aerogels: Curcumin Case Study, Molecules 25 (2020) 1187.

[26] A. Veronovski, G. Tkalec, Ž. Knez, Z. Novak, Characterisation of biodegradable pectin aerogels and their potential use as drug carriers, Carbohydr. Polym. 113 (2014) 272-278.

[27] S. Groult, T. Budtova, Tuning structure and properties of pectin aerogels, Eur. Polym. J. 108 (2018) 250-261.

[28] S. Groult, T. Budtova, Thermal conductivity/structure correlations in thermal super-insulating pectin aerogels, Carbohydr. Polym. 196 (2018) 73-81.

[29] S.H. Yalkowsky, Y. He, P. Jain, Handbook of Aqueous Solubility Data, CRC Press, Boca Raton, 2016.

[30] M. Johannsen, G. Brunner, Solubilities of the xanthines caffeine, theophylline and theobromine in supercritical carbon dioxide, Fluid Phase Equilib. 95 (1994) 215-226.

[31] D.R. Lide, CRC handbook of chemistry and physics, 87th ed., CRC Press, Boca Raton, 2006.

[32] C. Rudaz, R. Courson, L. Bonnet, S. Calas-Etienne, H. Sallee, T. Budtova, Aeropectin: fully biomass-based mechanically strong and thermal superinsulating aerogel, Biomacromolecules 15 (2014) 2188-2195.

[33] T. Mehling, I. Smirnova, U. Guenther, R.H.H. Neubert, Polysaccharide-based aerogels as drug carriers, J. Non-Cryst. Solids 355 (2009) 2472-2479.

[34] M. Grassi, I. Colombo, R. Lapasin, Experimental determination of the theophylline diffusion coefficient in swollen sodium-alginate membranes, J. Controlled Release. 76 (2001) 93-105.

[35] M. Grassi, G. Grassi, R. Lapasin, I. Colombo, Understanding Drug Release and Absorption Mechanisms: A Physical and Mathematical Approach, CRC press, 2006.

[36] M. Alnaief, I. Smirnova, Effect of surface functionalization of silica aerogel on their adsorptive and release properties, J. Non-Cryst. Solids 356 (2010) 1644-1649.

[37] I. Smirnova, J. Mamic, W. Arlt, Adsorption of drugs on silica aerogels, Langmuir 19 (2003) 8521-8525.

[38] I. Smirnova, S. Suttiruengwong, W. Arlt, Aerogels: tailor-made carriers for immediate and prolonged drug release, KONA Powder Part. J. 23 (2005) 86-97.

[39] S. Groult, S. Buwalda, T. Budtova, Pectin hydrogels, aerogels, cryogels and xerogels: Influence of drying on structural and release properties, Eur. Polym. J. 149 (2021) 110386.

[40] M.A. Marin, R.R. Mallepally, M.A. McHugh, Silk fibroin aerogels for drug delivery applications, J. Supercrit. Fluids 91 (2014) 84-89.

[41] X. Huang, C.S. Brazel, On the importance and mechanisms of burst release in matrix-controlled drug delivery systems, J. Controlled Release 73 (2001) 121-136.

[42] J. Siepmann, F. Siepmann, Mathematical modeling of drug delivery, Int. J. Pharm. 364 (2008) 328-343.

[43] P.L. Ritger, N.A. Peppas, A simple equation for description of solute release II. Fickian and anomalous release from swellable devices, J. Controlled Release 73 5 (1987) 37-42.

[44] R.W. Korsmeyer, R. Gurny, E. Doelker, P. Buri, N.A. Peppas, Mechanisms of solute release from porous hydrophilic polymers, Int. J. Pharm. 15 (1983) 25-35.

Supporting information for

Tuning bio-aerogel properties for controlling theophylline delivery.

Part 1: Pectin aerogels

*Sophie Groult, Sytze Buwalda, Tatiana Budtova**

MINES ParisTech, PSL Research University, Center for Materials Forming (CEMEF), UMR CNRS 7635, CS 10207, 06904 Sophia Antipolis, France

*Corresponding author: Tatiana Budtova

Tatiana.budtova@mines-paristech.fr

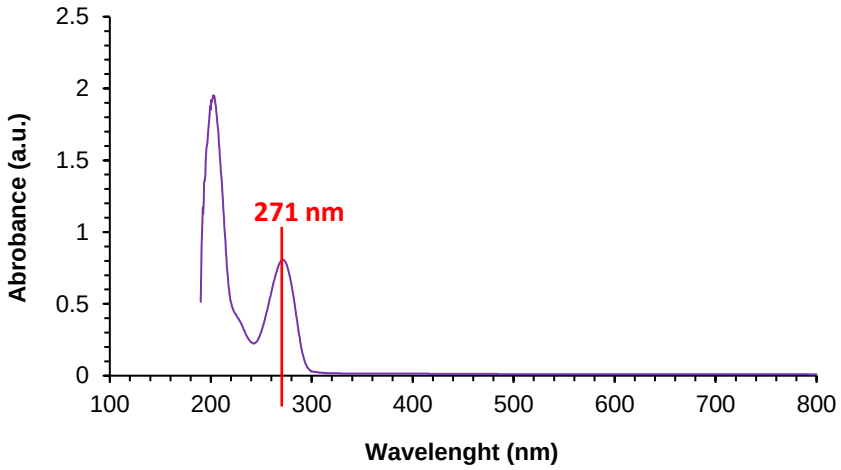

Figure S1.
Absorption spectrum of theophylline (0.0125 g/L in SIF).

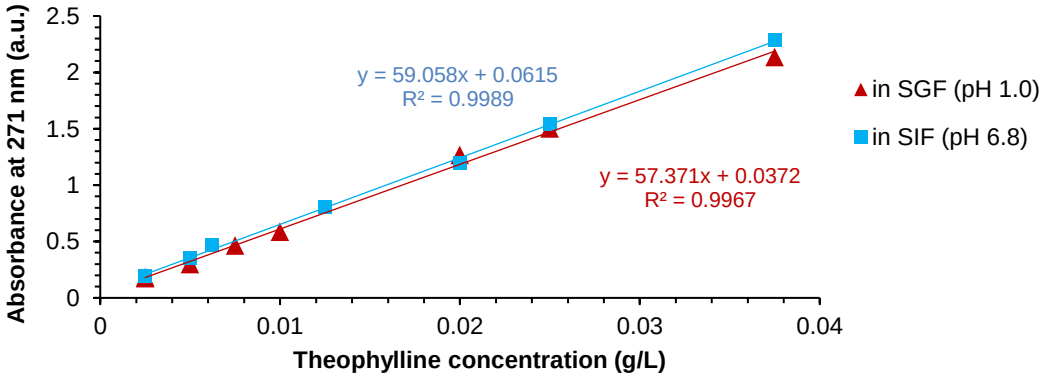

Figure S2.

Absorbance calibration curves (at 271 nm) for theophylline dissolved in SGF (pH 1.0) and in SIF (pH 6.8). Straight lines are linear regressions of the data.

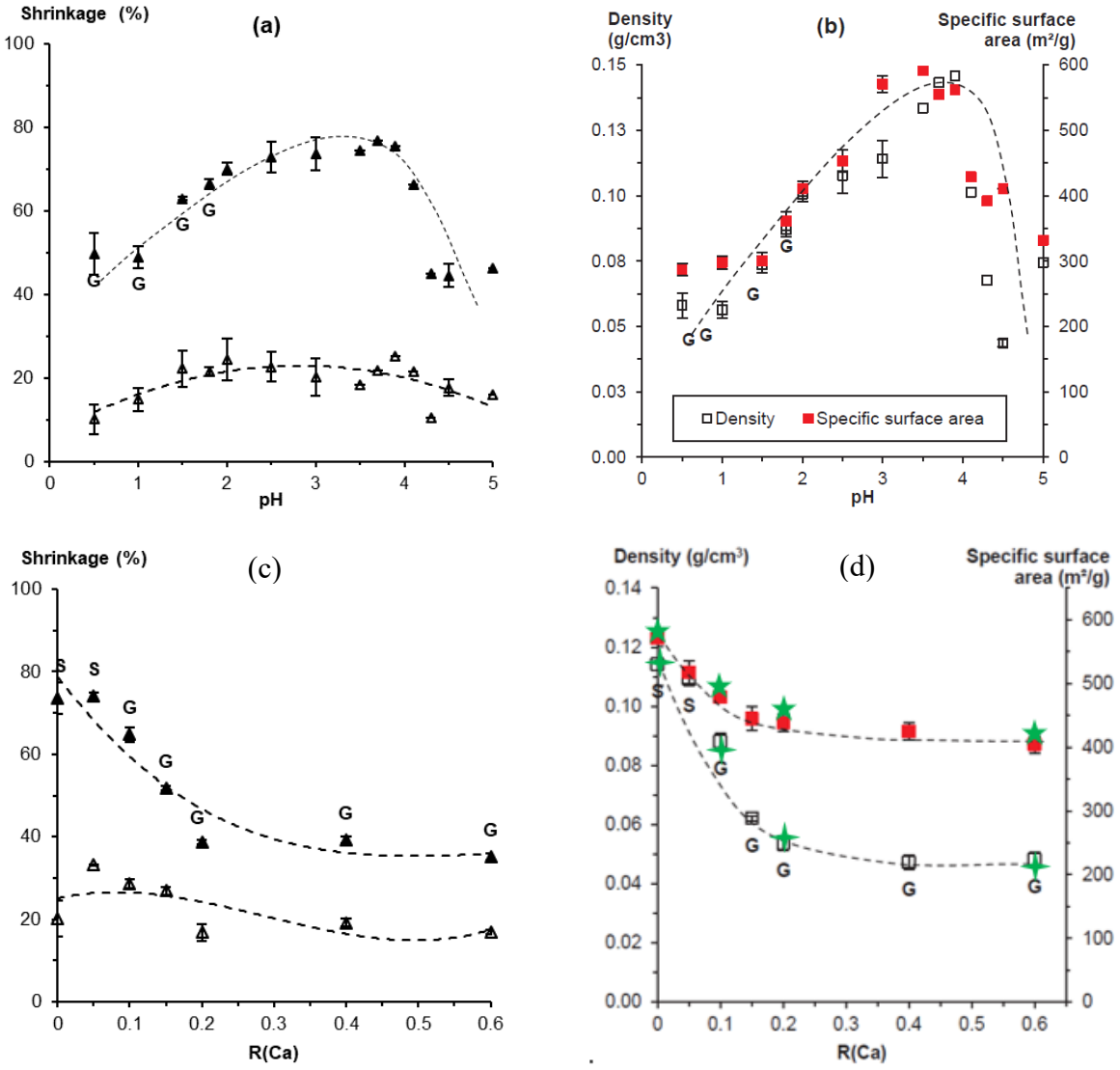

Figure S3.

Volumetric shrinkage (a, c) after solvent exchange (open points) and after sc-drying (filled points); density (b, d, open points) and specific surface area (b, d, filled points) of neat pectin aerogels made from 3 wt% solutions as a function of pH (no calcium) (a, b) and molar ratio R(Ca) (pH 3) (c, d). The state of the matter before solvent exchange is noted "G" for gel, the rest are solutions.

Figures (a, b, c) are reprinted from Eur. Polym. J. 108 (2018) 250-261, S. Groult, T. Budtova, "Tuning structure and properties of pectin aerogels", Copyright 2018, with permission from Elsevier; in (d) data are taken from ref.1 and the stars are data obtained in this work for theophylline loaded aerogels of the same formulation. Dashed lines are given to guide the eye.

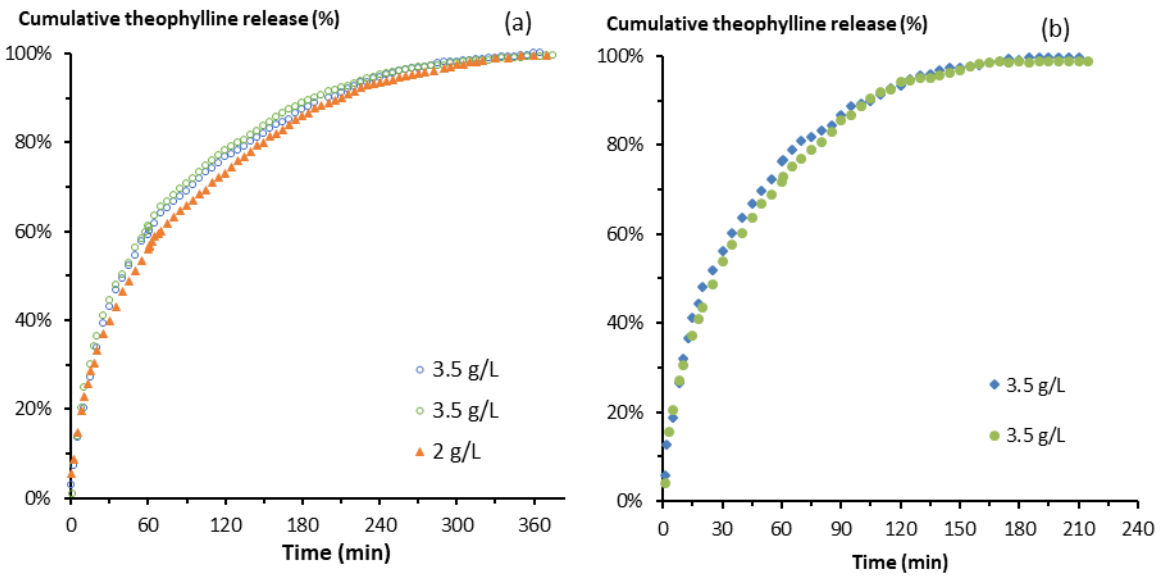

Figure S4.

Example of results reproducibility for theophylline release over time from pectin aerogels prepared from (a) 6 wt% pectin dissolved at pH 3.0 in the absence of calcium, theophylline concentration in the impregnation solution was 2 and 3.5 g/L; (b) 3 wt% pectin dissolved at pH 3 in the absence of calcium, theophylline concentration in the impregnation solution was 3.5 g/L.

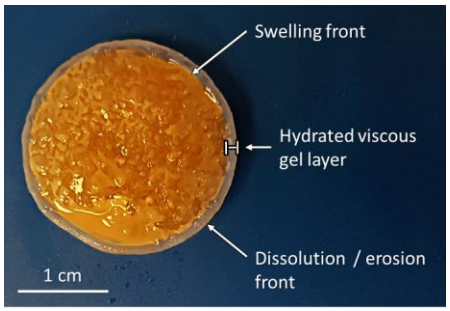

Figure S5.

Picture of a pectin aerogel after being immersed in SGF at 37 °C for 45 min. The aerogel was prepared from 6 wt% pectin dissolved at pH 3.0 in the absence of calcium.

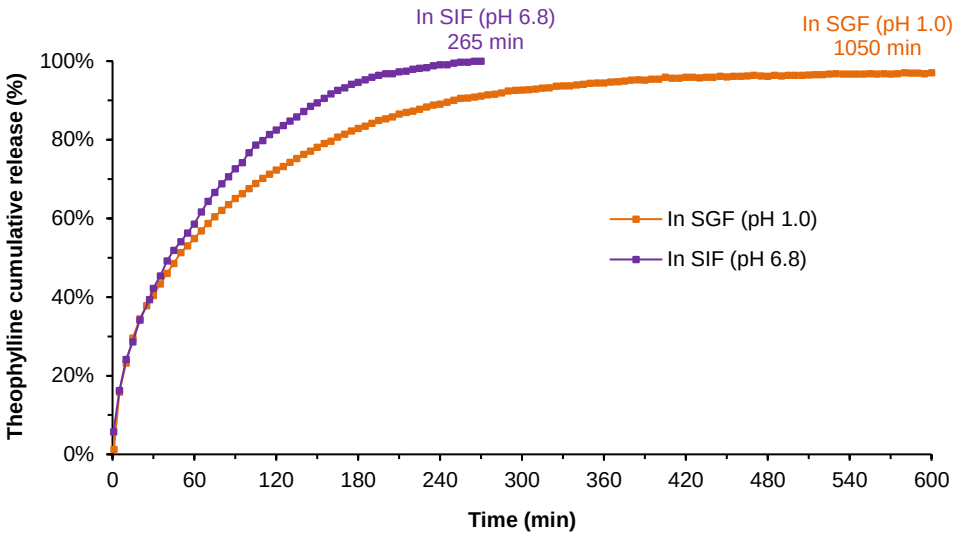

Figure S6.

Theophylline cumulative release (%) from pectin aerogels (6 wt% dissolved at pH 3.0 without calcium) over time in either SGF medium (pH 1.0) or in SIF medium (pH 6.8) at 37 °C during the whole dissolution testing.

Table S1. Summary of release kinetics models for solid polymer matrices; *Q(t)* is the normalized cumulative drug released at time *t*

Model	**Equation**	**Comment**
Higuchi	$Q(t) = K_H\sqrt{t}$	K_H is Higuchi constant which includes pores' tortuosity, initial concentration of the drug, its solubility, etc
Hixson-Crowell	$\sqrt[3]{1 - Q(t)} = 1 - k_\beta . t$	k_β is a constant
Hopfenberg	$Q(t) = K_G^2 t^2 - K_G t$ (for cylinders)	K_G is a constant
Korsmeyer–Peppas	$Q(t) = K_{KP} t^n$ (for $Q(t) < 60\%$)	K_{KP} is a constant
Peppas–Sahlin	$Q(t) = K_\mathrm{F} t^m + K_\mathrm{R} t^{2m} = F + R$ $\frac{R}{F} = \frac{K_R}{K_F} t^m$ (for $Q(t) < 60\%$)	K_F is diffusion constant, K_R is relaxation constant, m is Fickian diffusion exponent, R is relaxational and F Fickian contributions, respectively
Gallagher–Corrigan	$\mathrm{Q(t)} = = F_{max}[1 - \exp(-k_b t)] + (F_{max} - F_b)\left[\frac{\exp(k_\mathrm{e} t - k_\mathrm{e} t_\mathrm{max})}{1 + \exp(k_\mathrm{e} t - k_\mathrm{e} t_\mathrm{max})}\right]$	F_{max} is the maximum fraction of drug released during the total time period; F_b fraction of drug released during the initial burst phase, t_{max} the time to the maximum drug release rate, and k_b and k_e are the first order kinetic coefficients of the first (burst) phase and of the second (erosion-controlled) phase, respectively

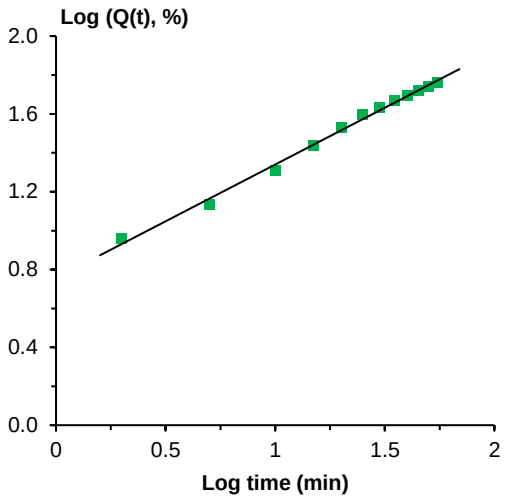

Figure S7.

Experimental data (first 60 % drug release) from Figure 6a fitted in the Korsmeyer-Peppas model. An *n* exponent value (Table S1) of 0.58 was obtained from the slope of the regression line with $R^2 = 0.9945$.

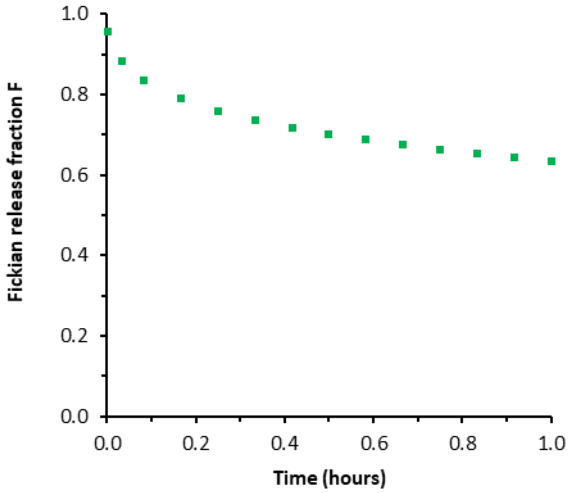

Figure S8.

Example of the Fickian release fraction F from Peppas-Sahlin model (see Table S1) as a function of time for the data from Figure 6a: aerogels were disks with the aspect ratio (diameter to thickness) between 2.3 and 2.5, corresponding to a Fickian diffusional exponent *m* (see Table S1) of approximately 0.43 [2]. Diffusional and relaxational constants are $K_F \sim 0.388\ min^{-0.43}$ and $K_R \sim 0.223\ min^{-0.86}$, respectively.

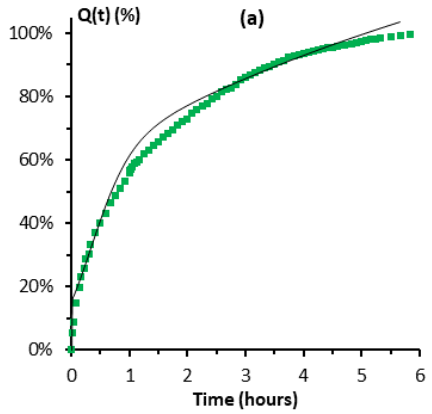

(b)

Parameter	**value**
Burst constant k_b (h^{-1})	0.101
Erosion constant k_e (h^{-1})	3.095
Time to max. drug release rate t_{max} (h)	0.350
Drug fraction released in initial burst phase F_b	0.384

Figure S9.

(a) Experimental data (points) from Figure 6a fitted in the Gallagher-Corrigan model (black line, $F_{max} = 1$); (b) parameters of the model obtained via least squares fitting ($R^2 = 0.99$).

(a)

Pectin solution pH	1.2 (curve 1)	2.0 (curve 2)	3.0 (curve 3)
Aerogel density (g/cm^3)	0.105	0.136	0.181
Fickian coefficient K_F ($h^{-0.43}$)	0.476	0.468	0.414
Relaxational coefficient K_R ($h^{-0.86}$)	0.393	0.262	0.152
R^2	0.997	0.993	0.996

(b)

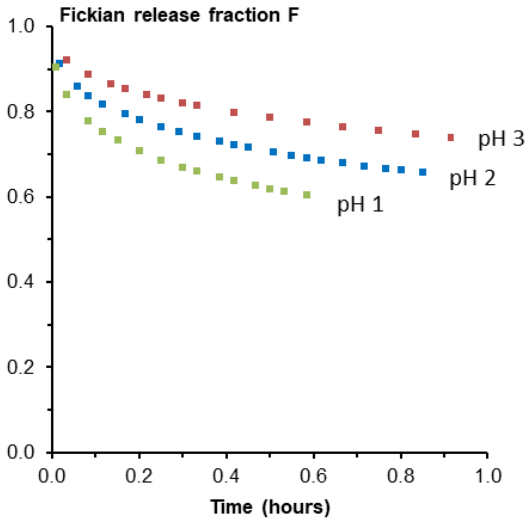

Figure S10.

(a) Estimation of the Peppas-Sahlin parameters after fitting experimental data (first 60% of released drug) from Figure 7a in the Peppas-Sahlin model, using a Fickian diffusional exponent *m* of 0.43. (b) Fickian release fraction (F) as a function of time, as determined with the parameters in (a) for release from a flat cylinder with $m \sim 0.43$. Each symbol corresponds to an experimental point of Figure 7a recalculated using the Peppas-Sahlin model.

(a)

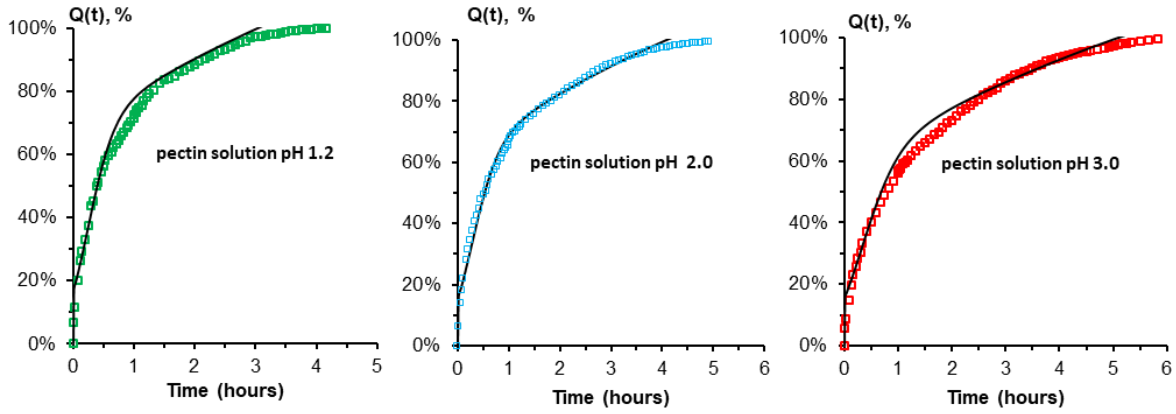

(b)

Pectin solution pH	1.2	2.0	3.0
Aerogel density (g/cm^3)	0.105	0.136	0.181
Burst constant k_b (h^{-1})	0.129	0.121	0.104
Erosion constant k_e (h^{-1})	4.612	3.907	3.005
Time to max. drug release rate t_{max} (h)	0.242	0.2823	0.340
Drug fraction released in initial burst phase F_b	0.324	0.390	0.414
R^2	0.99	0.992	0.991

Figure S11.

(a) Experimental data from Figure 7a fitted in the Gallagher-Corrigan model. (b) Parameters of the model obtained via least squares fitting.

(a)

R(Ca)	0	0.1	0.2	0.6
Aerogel density (g/cm^3)	0.118	0.085	0.056	0.044
Fickian coefficient K_F ($h^{-0.43}$)	0.3516	0.3767	0.3350	0.5128
Relaxational coefficient K_R ($h^{-0.86}$)	0.6611	0.5183	0.3347	0.1985
R^2	0.9930	0.9942	0.9930	0.9948

(b)

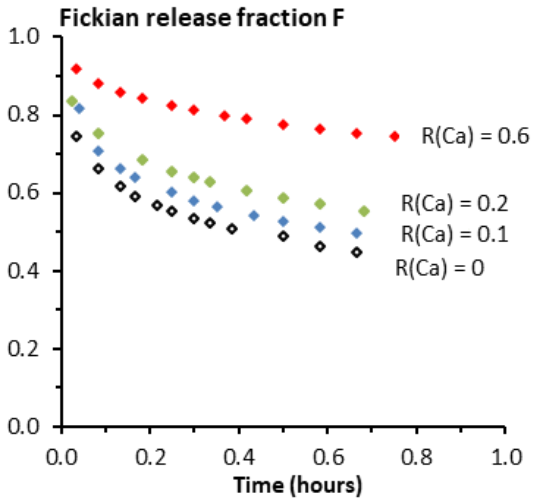

Figure S12.

(a) Estimation of the Peppas-Sahlin parameters after fitting experimental data (first 60% of released drug) from Figure 9a in the Peppas-Sahlin model, using a Fickian diffusional exponent *m* of 0.43. (b) Fickian release fraction (F) as a function of time, as determined with the parameters in (a) for release from a flat cylinder with $m \sim 0.43$.

(a)

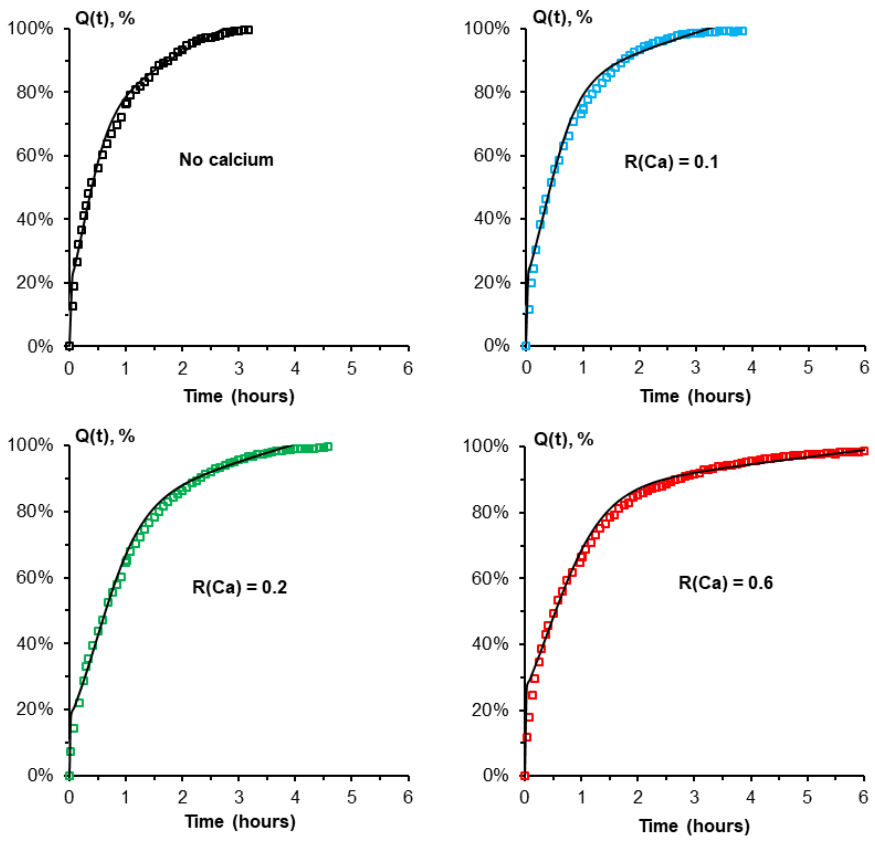

(b)

R(Ca)	0	0.1	0.2	0.6
Aerogel density (g/cm^3)	0.118	0.085	0.056	0.044
Burst constant k_b (h^{-1})	0.1402	0.0718	0.0651	0.0241
Erosion constant k_e (h^{-1})	4.1889	3.3080	2.5492	2.0625
Time to max. drug release rate t_{max} (h)	0.2413	0.3169	0.4905	0.4076
Drug fraction released in initial burst phase, F_b	0.3164	0.2049	0.2286	0.1444
R^2	0.992	0.9911	0.9937	0.9910

Figure S13.

(a) Experimental data from Figure 9a fitted in the Gallagher-Corrigan model. (b) Parameters of the model obtained via least squares fitting.

References

[1] S. Groult, T. Budtova, Tuning structure and properties of pectin aerogels, Eur. Polym. J. 108 (2018) 250-261.

[2] N.A. Peppas, J.J. Sahlin, A simple equation for the description of solute release. III. Coupling of diffusion and relaxation, Int. J. Pharm. 57 (1989) 169-172.